Monthly Notices
of the
ROYAL ASTRONOMICAL SOCIETY

MNRAS **480,** 1656–1665 (2018) doi:10.1093/mnras/sty1882

# The solar-like 'Second Spectrum' and polarized metal lines in the emission of the post-AGB binary 89 Herculis

F. Leone,[1,2]★ M. Gangi,[1,2] M. Giarrusso,[3] C. Scalia,[2] M. Cecconi,[4] R. Cosentino,[4] A. Ghedina,[4] M. Munari[2] and S. Scuderi[2]

[1] *Università di Catania, Dipartimento di Fisica e Astronomia, Sezione Astrofisica, Via S. Sofia 78, I–95123 Catania, Italy*
[2] *INAF – Osservatorio Astrofisico di Catania, Via S. Sofia 78, I–95123 Catania, Italy*
[3] *INFN – Laboratori Nazionali del Sud, Via S. Sofia 62, I-95123 Catania, Italy*
[4] *INAF – Fund. Galileo Galilei, Rambla José Ana Fernández Perez 7, 38712 Breña Baja (La Palma), Canary Islands, Spain*

Accepted 2018 July 10. Received 2018 May 23; in original form 2017 June 26

## ABSTRACT

We studied the polarized spectrum of the post-AGB binary system 89 Herculis on the basis of data collected with the high-resolution Catania Astrophysical Observatory Spectropolarimeter, HArps-North POlarimeter and Echelle SpectroPolarimetric Device for the Observation of Stars. We find the existence of linear polarization in the strongest metal lines in absorption and with low excitation potentials. Signals are characterized by complex $Q$ and $U$ morphologies varying with the orbital period. We rule out magnetic fields, continuum depolarization due to pulsations and hot spots as the possible origin of this 'Second Solar Spectrum'-like behaviour. The linear polarization we detected in the CaII 8662-Å line is clear evidence of optical pumping polarization and rules out scattering polarization from free electrons of the circumbinary environment. In the framework of optical pumping due to the secondary star, the observed periodic properties of the spectral line polarization can be justified by two jets, with a flow velocity of a few tens of km s$^{-1}$, at the basis of that hourglass structure characterizing 89 Herculis. We also discovered linear polarization across the emission profile of metal lines. Numerical simulations show that these polarized profiles could be formed in an undisrupted circumbinary disc rotating at $\leq$10 km s$^{-1}$ and with an orientation in the sky in agreement with optical and radio interferometric results. We conclude that the study of aspherical envelopes, the origin of which is not yet completely understood, of PNe and already present in post-AGBs can benefit from high-resolution spectropolarimetry and that this technique can shape envelopes still too far away for interferometry.

**Key words:** atomic process – polarization – techniques: polarimetric – stars: AGB and post-AGB – stars: individual: 89 Hercircumstellar matter.

## 1 INTRODUCTION

Photopolarimetry by Kruszewski, Gehrels & Serkowski (1968) has shown that the Mira variable stars are characterized by a certain degree of linear polarization changing with wavelength and time. By means of spectropolarimetry at low resolution, McLean & Coyne (1978) have pointed out a high polarization degree, up to 7 per cent, across Balmer lines of Mira itself. Harrington & Kuhn (2009b,a) and Lèbre, Fabas & Gillet (2011) have shown that such a property is often present in the Balmer lines of evolved stars. The existence of linear polarization across individual metal lines in absorption has been reported for the Mira star $\chi$ Cygni by Lèbre et al. (2014) and for the red supergiant Betelgeuse by Aurière et al. (2016). Using least-squares deconvolution (LSD: Donati et al. 1997), evidence of linear polarization was found byTessore, Lèbre & Morin (2015) in the spectral lines of the RV Tau variable R Scuti and Sabin, Wade & Lèbre (2015) in the lines of the RV Tau variable U Monoceroti, as well in the post-AGB star 89 Herculis.

It appears that evolved stars can be characterized by the so called 'Second Solar Spectrum', consisting of spectral lines partially in absorption and partially in emission when observed with high-resolution linear spectropolarimetry (Stenflo 1982). This spectrum in polarized light has represented the observational basis for comprehension of the most external layers of the Sun and now its discovery in evolved stars opens a new perspective on our understanding of stellar evolution. In general, polarization across spectral lines is expected to trace and shape the envelopes of the final stellar stages,

★ E-mail: fleone@oact.inaf.it

the departure from spherical symmetry of which is still a matter of discussion (Martínez González et al. 2015). Despite many theories invoking magnetic fields to explain the rich variety of aspherical components observed in planetary nebulae (PNe) (see the review by Balick & Frank 2002), no direct observational evidence of such fields has yet been established (Leone et al. 2011, 2014; Jordan et al. 2012; Asensio Ramos et al. 2014; Sabin et al. 2015). The presence of rotating circumbinary discs is also a fundamental problem in understanding post-asymptotic giant branch (post-AGB) evolution (Bujarrabal et al. 2007).

In this context, we report on one of the most well-known long-term variables: 89 Herculis (Section 2). A study based on high-resolution linear spectropolarimetry (Section 3) is carried out, with the aim of pointing out any possible envelope asymmetry already present in the post-AGB phase before the PN phase. In Section 3.1, in analogy with the 'Second Solar Spectrum', we present the 'Second Stellar Spectrum' of 89 Her and its periodic variability . In Section 3.2, we present the polarization of metal lines in emission from the circumbinary envelope and relate their properties to the geometry and dynamics of the emitting region. In Section 4, we analyse the possible origins of this polarization. Finally, we present our conclusions in Section 5.

## 2 89 HERCULIS

Classified as an F2 Ib C supergiant by Gray & Garrison (1989), 89 Herculis (HR 6685, HD 163506) is the prototype of the new class, introduced by Waters et al. (1993), of post-AGB binaries surrounded by a circumbinary dust disc. The ephemeris of this binary system was determined by Waters and coworkers from radial velocities (RV):

$$JD(\mathrm{RV}_{\max}) = 2\,446\,013.72(\pm 16.95) + 288.36(\pm 0.71) \text{ days.} \quad (1)$$

Furthermore, the primary component of 89 Her pulsates with a period of 63.5 days (Arellano Ferro 1984).

Interferometric data of 89 Her have been interpreted by Bujarrabal et al. (2007) as suggestive of two nebular components: an expanding hourglass structure and an unresolved circumbinary Keplerian disc. Bujarrabal and coworkers concluded that the hourglass axis is tilted with respect to the line of sight (LoS) of $\theta_{\mathrm{LoS}} = 15^{\circ}$ with a position angle $\theta_{\mathrm{PA}} = 45^{\circ}$.

From the basis of time-resolved broad-band photopolarimetry, Akras et al. (2017) concluded that 89 Her is an intrinsic unpolarized source in the visible range.

## 3 OBSERVATIONAL DATA

From 2014 June–2016 October, we have performed high-resolution linear spectropolarimetry of 89 Her with the high-resolution Catania Astrophysical Observatory Spectropolarimeter (CAOS: $R =$ 55 000, Leone et al. 2016a) at the 0.91-m telescope of the stellar station of the Catania Astrophysical Observatory (G. M. Fracastoro Stellar Station, Serra La Nave, Mount Etna, Italy). A spectrum in linearly polarized light was acquired on 2017 May 27 with the HArps-North POlarimeter (HANPO: $R =$ 115 000, Leone et al. 2016b) of the Telescopio Nazionale Galileo (Roque de Los Muchachos Astronomical Observatory, La Palma, Spain). Data were reduced and Stokes *Q/I*, *U/I* and null spectra *N* obtained according to the procedures described in Leone et al. (2016a). The null spectra check for the presence of any spurious contribution to the polarized spectra and errors in the data reduction process.

**Table 1.** Logbook of observations. The achieved signal-to-noise ratio (S/N) is determined from null LSD spectra.

| HJD 240 0000+ | S/N | Instr. | HJD 240 0000+ | S/N | Instr. |
|---|---|---|---|---|---|
| 53604.753 | 11300 | ESP | 55102.832 | 5200 | ESP |
| 53775.115 | 10500 | ESP | 55109.823 | 12400 | ESP |
| 53777.096 | 19400 | ESP | 56816.515 | 3000 | CAOS |
| 53961.777 | 21800 | ESP | 56862.456 | 2300 | CAOS |
| 54372.821 | 23900 | ESP | 56863.347 | 2400 | CAOS |
| 54877.099 | 4300 | ESP | 56876.340 | 3500 | CAOS |
| 54878.132 | 10700 | ESP | 56894.309 | 4200 | CAOS |
| 54880.076 | 14700 | ESP | 56897.301 | 4100 | CAOS |
| 54954.125 | 12900 | ESP | 56898.274 | 4300 | CAOS |
| 54955.849 | 10600 | ESP | 56904.313 | 3700 | CAOS |
| 54958.121 | 14000 | ESP | 57582.248 | 3700 | CAOS |
| 54959.874 | 8000 | ESP | 57666.248 | 2900 | CAOS |
| 55081.874 | 3000 | ESP | 57900.602 | 4300 | HANPO |

In addition, reduced spectropolarimetric data of 89 Her have been retrieved from the Canadian Astronomy Data Centre. Spectra were collected from 2005–2009 at the 3.6-m Canada–France–Hawaii Telescope with the Echelle SpectroPolarimetric Device for the Observation of Stars (ESPaDOnS: $R =$ 68 000, Donati et al. 2006). The logbook of observations is given in Table 1.

The final observational data consist of time-resolved spectra of 89 Her with evidence of polarization across the profile of metal lines. We found large differences between absorption and emission lines.

### 3.1 Polarized metal lines in absorption

Sabin et al. (2015) discovered evidence of linear polarization in the Stokes *Q/I* and *U/I* LSD profiles of 89 Her spectra recorded with ESPaDOnS on 2006 February 8. We found that all the archived ESPaDOnS spectra of 89 Her, spanning about 1400 days, are characterized by about 50 spectral lines of iron-peak elements in absorption, the Stokes *Q/I* and *U/I* profiles of which appear as non-null and variable in time, despite photon noise. Fig. 1 provides an example of such variable signals for transitions of Fe II, Cr II and Ti II. In any spectrum, Stokes profiles scale with the line depth irrespective of wavelength (Fig. 2). We have then selected in the 400–700nm range, common to the three spectropolarimeters, a set of about 1000 spectral lines of iron-peak elements, the Stokes *I* residual of which is larger than 0.2, to obtain Stokes *Q/I* and *U/I* LSD profiles. Fig. 3 shows a comparison between the ESPaDOnS-LSD and Fe II 4508.288-Å profiles on three different dates.

In CAOS spectra of 89 Her, we do not find any direct evidence of polarization. After numerical simulations showing that ESPaDOnS Stokes *Q/I* and *U/I* profiles would be hidden in the signal-to-noise ratio (S/N) of CAOS spectra, we have successfully constructed the CAOS-LSD profiles from the spectral line list we selected for the ESPaDOnS-LSD. For consistency, the HANPO-LSD Stokes profiles were also based on the same list of spectral lines. The complete collection of variable Stokes *Q/I* and *U/I* LSD profiles is shown in Fig. 4. S/N values achieved in null LSD profiles are given in Table 1.

We then performed a time analysis of the total polarization measured across the LSD profiles. The Scargle (1982) periodogram, CLEANED following Roberts, Lehar & Dreher (1987), presents the highest peak at 294 ± 5 days, which is coincident within the errors with the orbital period (Fig. 5). For this reason, hereafter we

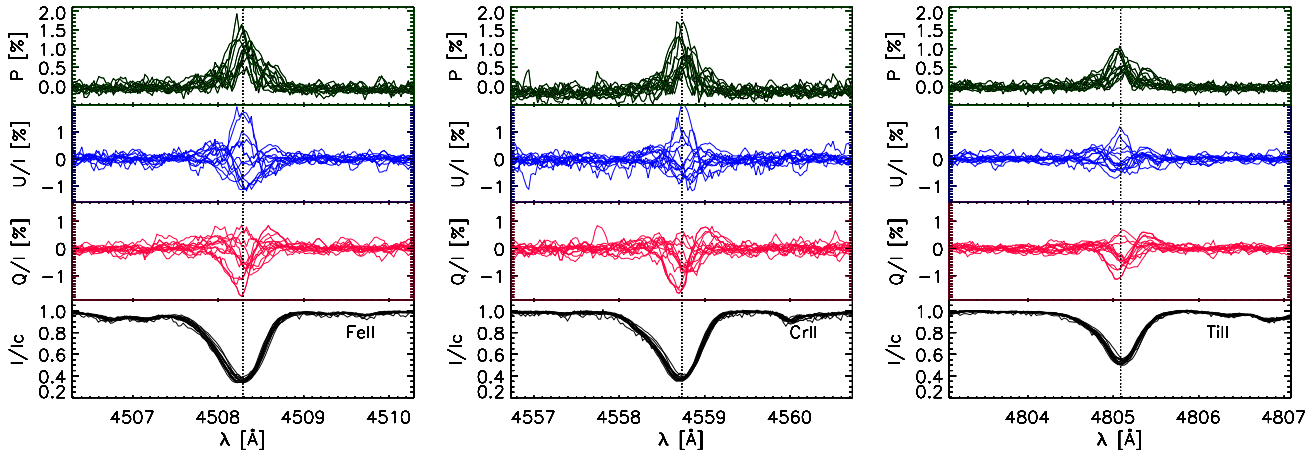


**Figure 1.** All 15 ESPaDOnS Stokes *I*, *Q*/*I*, *U*/*I* profiles and polarization ($P = \int \sqrt{(Q/I)^2 + (U/I)^2}\,\mathrm{d}\lambda$) for the Fe II 4508.288-Å, Cr II 4558.783-Å and Ti II 4805.085-Å lines. Data collected between 2005 and 2009 present a clearly linear polarization and a significant morphological variability in time.

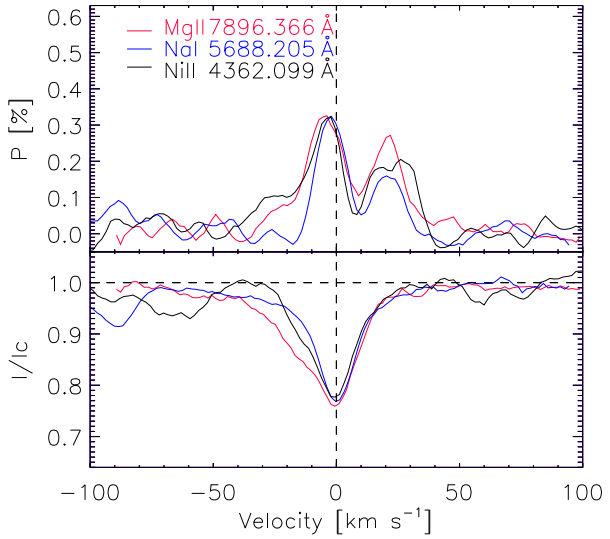


**Figure 2.** Examples of spectral lines with equal depth showing that, within the errors, polarization does not depend on wavelength.

will adopt the ephemeris by Waters et al. (1993) (equation 1). Fig. 5 shows how the total polarization changes with orbital period. A similar variability cannot be statistically confirmed for the equivalent widths, for which a sinusoidal fit gives an amplitude of $10 \pm 9$ mÅ.

### 3.2 Polarized metal lines in emission

Discovered by Osmer (1968), more than 300 weak metal lines in emission have been identified by Kipper (2011) in the spectrum of 89 Her. Kipper pointed out that these lines (1) present the velocity of the binary system, (2) are due to neutral metals with rather low (<6 eV) excitation levels and (3) are not due to forbidden and ionic transitions. Kipper concluded that these emission lines are formed in the circumbinary disc. Already, Waters et al. (1993) have interpreted these weak, neutral or low-excitation-level emission lines of metals as proof of collisionally excited interaction between the stellar wind and the circumbinary disc.

We have analysed the polarization properties of the emission metal lines crowding the spectrum of 89 Her and found, as a general rule, that they present (left panel of Fig. 6) about 1 per cent polarization, fully stored in the Stokes *U*/*I* profile. However, a few emission lines appear to show the opposite behaviour (right panel of Fig. 6), to be confirmed with further observations.

## 4 ORIGIN OF THE LINEAR POLARIZATION OF METAL LINES

Basic mechanisms forming the basis of the observed linear polarization in metal lines are as follows.

(i) The presence of a polarized continuum, e.g. due to scattering by grains, molecules (Rayleigh scattering) or free electrons (Thomson scattering). In this case, thermal recombination radiation would appear as spectral lines unpolarizing the continuum, an effect that at high spectral resolution, when the continuum polarization is settled at zero, results in apparently polarized spectral lines.

(iii) Fluorescence in a volume without spherical symmetry (e.g. disc, bipolar flux) in the presence of free electrons capable of scattering radiation.

(iv) Anisotropic radiation on emitting atoms, not necessarily in excited Zeeman states (Landi Degl'Innocenti & Landolfi 2004; Trujillo Bueno 2005; Yan & Lazarian 2008).

### 4.1 Metal lines in emission

Despite the Hillen et al. (2013) detection of a 35–40 per cent optical circumstellar flux contribution to the 89 Her luminosity, the previous point (1) can be ruled out for polarized metal lines in emission. The observed continuum of 89 Her is unpolarized (Akras et al. 2017).

As to emission lines, regardless of the proposed (Waters et al. 1993) mechanisms for their origin, polarized profiles are expected from rotating discs (Vink, Harries & Drew 2005) in the presence of free electrons. We have carried out numerical computations with the STOKES code and found that observations are justified by an open undisrupted disc slightly tilted towards the line of sight and rotating at $\leq$ 10 km s$^{-1}$, see Fig. 7. This value is in agreement with the conclusion of Bujarrabal et al. (2007) that the characteristic rotation would be $\sim$8 km s$^{-1}$. We adopted a density of scattering electrons equal to $10^{10}$ cm$^{-3}$, an external radius of 10 au and a PA of the circumbinary disc equal to 45°.

In the literature, indirect evidence of free electrons in the circumbinary disc of 89 Her is a necessity of the H$^-$ continuum opacity, in order to justify the observed spectral energy distribution (Hillen

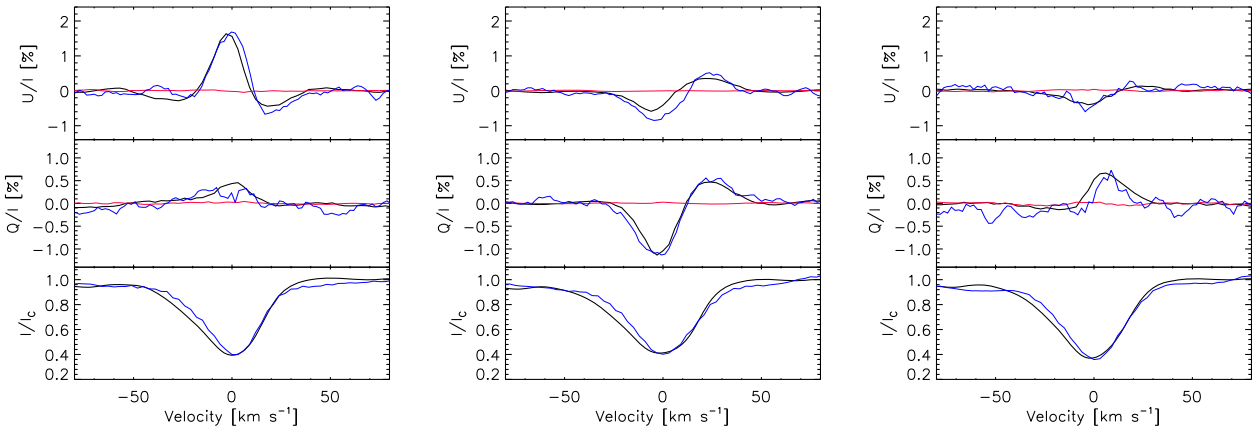


**Figure 3.** ESPaDOnS: comparison between the Stokes parameters of the Fe II 4508.288-Å (thin, blue) line and LSD profiles (thick, black). LSD null polarization is in red. From the left, spectra were acquired using HJD 53604.753, 53961.777 and 54878.132 data.

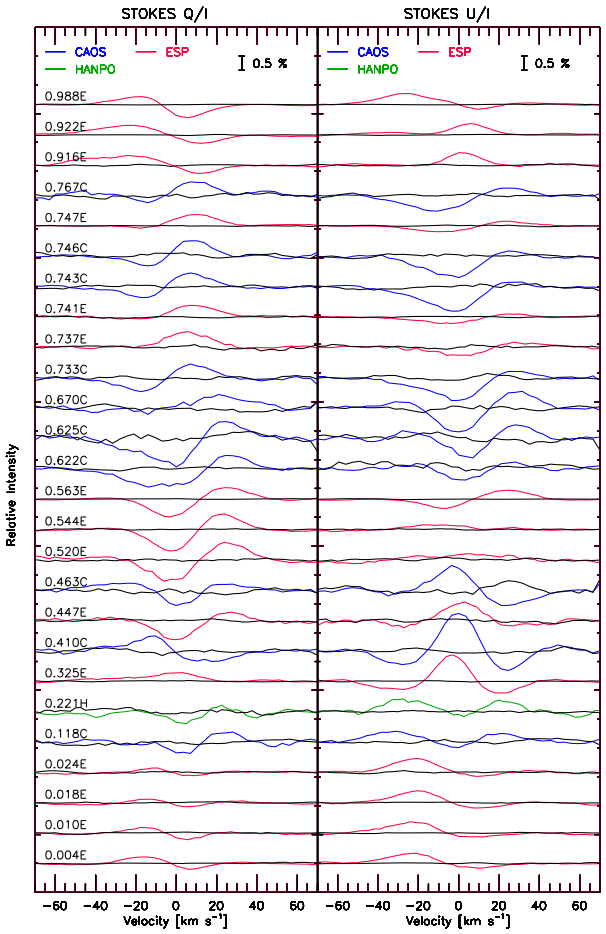


**Figure 4.** Observed Stokes *Q/I* and *U/I* LSD profiles of 89 Her. Null polarization in black. Profiles are ordered according to the orbital phase computed with the equation (1) ephemeris and arbitrarily shifted for better visualization. After the phase value, 'E' means that the spectra were obtained with ESPaDOnS, 'C' with CAOS and 'H' with HANPO.

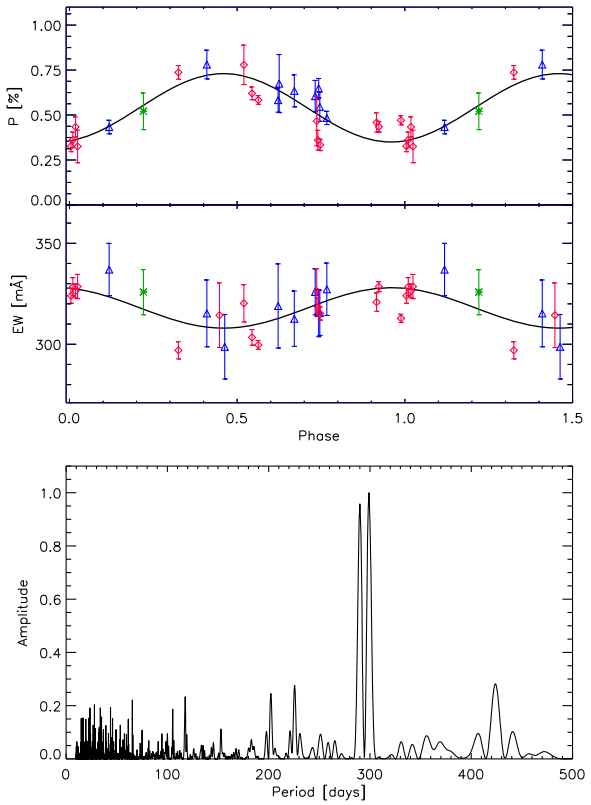


**Figure 5.** Bottom panel: CLEANED (Roberts et al. 1987) periodogram (Scargle 1982) of LSD polarization of 89 Her. The highest peak is close to the 288.36-day orbital period, while no power is present at the pulsation period of 63.5 days. Variations of the total polarization *P* (top panel) and equivalent width (EW, middle panel) of LSD profiles are plotted according to the orbital phase; a sine fit of variability is also shown. Symbols are as follows: ⋄ for ESPaDOnS data, △ for CAOS data and ∗ for HANPO data.

et al. 2013), a result that rules out the presence of scattering on grains within the circumbinary disc. We also note that mass loss ($\sim 10^{-8}\,M_\odot\ yr^{-1}$, Osmer 1968) from the primary star, responsible for the observed H$\alpha$ P Cygni profile, could be a continuous source of free electrons for the low-temperature circumbinary disc.

The observed Stokes *U/I* profiles do not rule out a possible variability with orbital period (Fig. 6). Further observations are necessary to clarify this possibility and eventually help us understand better the role of tidal forces induced by orbiting components on the circumbinary disc.

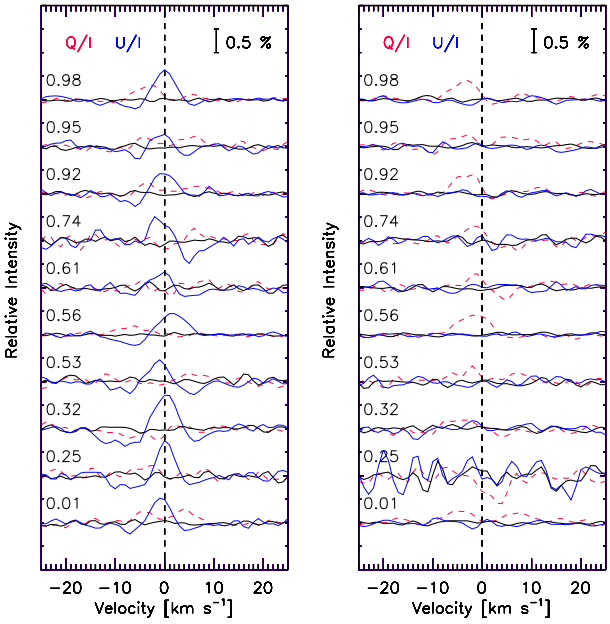


**Figure 6.** For any ESPaDOnS spectrum, we plot the average Stokes profiles of metal lines in emission. Phase is computed with the orbital ephemeris given in equation (1) (Waters et al. 1993). Most cases (left panel) present Stokes *U*/*I* (solid blue) profiles clearly different from zero and almost null Stokes *Q*/*I* (dashed red) profiles. A few others are characterized by a null Stokes *U*/*I* and possibly non-null Stokes *Q*/*I* profile (right panel).

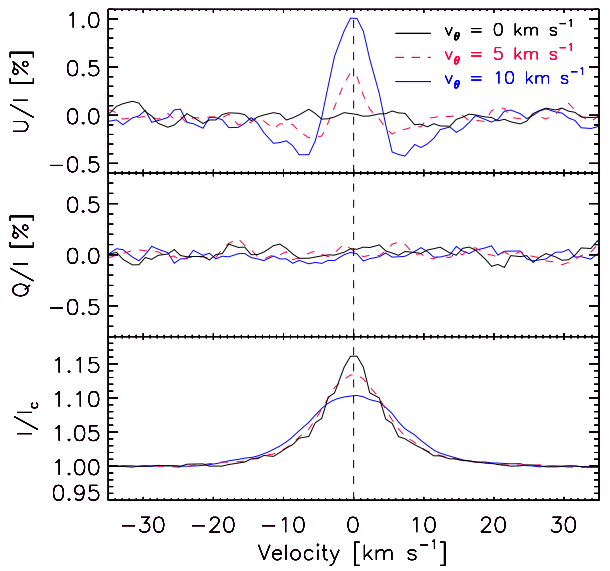


**Figure 7.** Polarization of a spectral line emitted from a 30° open undisrupted disc seen at $\cos(\theta) = 0.85$. The black solid line is for a non-rotating disc, the red dashed line for a disc with rotational velocity $v_\theta = 5\,\mathrm{km\,s^{-1}}$ and the blue dashed solid line for a disc with $v_\theta = 10\,\mathrm{km\,s^{-1}}$. To justify the null Stokes *Q* profiles, a PA=45° has been assumed.

## 4.2 Metal lines in absorption

The consideration that the polarization of metal lines in emission does not vary with the orbital period implies that the phenomenon responsible for the polarization of metal lines in absorption is on a scale not larger than the circumbinary disc and is related to the presence of the secondary. Here, we will consider, one by one, the possible mechanisms.

### *4.2.1 Magnetic fields*

Since Wade et al. (2000) and Bagnulo et al. (2001), linearly polarized metal lines have been observed in the spectra of magnetic chemically peculiar stars (Wolff 1983 still offers a complete and gentle introduction to this class of star) and are ascribed to the Zeeman effect. The presence of magnetic fields on the surface of 89 Her has been ruled out by Sabin et al. (2015), who detected no Stokes *V* signal across the LSD line profile (see their figure 1) and established an upper limit of 10 G on the effective magnetic field, which is by definition the average over the visible stellar disc of longitudinal components of the field (Babcock 1947).

With CAOS, we have also performed circular spectropolarimetry of 89 Her for HJD 56853.535 and an upper limit of 50 G has been estimated for the effective field from the Stokes *V* and *I* LSD profiles. The field has been measured with the moment technique, as in Leone & Catanzaro (2004). In principle, a linear polarization in spectral lines associated with a null circular polarization is possible for a purely transverse field. However, for a large-scale organized stellar magnetic field of a rotating star, even if the average of the longitudinal components across the visible stellar disc is null, Stokes *V* profiles are different from zero. We agree with the Sabin et al. (2015) conclusion and exclude the possibility that we are recording the linear polarization of Zeeman components.

### *4.2.2 Stellar continuum polarization*

**Stellar pulsations**

Odell (1979) first introduced the idea that stars with non-radial pulsations show a periodically variable polarization due to the photospheric electron-scattering opacity; he then observed linked photopolarimetric variability with an amplitude of 0.045 per cent in the star BW Vul (Odell 1981). Fabas, Lèbre & Gillet (2011) have associated the variable polarization presented by the Balmer lines of the pulsating o Ceti with the propagation of shock waves. Later, Lèbre et al. (2014) observed variable polarization in the metal lines of the Mira star $\chi$ Cygni and the RV Tauri star R Sct and they related the polarization to global asymmetry at the photospheric level induced by pulsations.

We can rule out the possibility that the metal-line polarization of 89 Her is a consequence of pulsations, simply because the observed polarization is not variable with the 63.5-day pulsation period but rather with the orbital period; see Fig. 5.

**Hot spots**

Schwarz & Clarke (1984) and Clarke & Schwarz (1984) have shown that the variable photopolarimetric data of Betelgeuse, with particular reference to the TiO band, can be a consequence of wavelength-independent (e.g. Thomson) scattering and temporal evolution of hot spots. Extending Clarke and Schwarz's interpretation, Aurière et al. (2016) suggested that the linear polarization observed in the spectral line of Betelgeuse is indeed an effect of the depolarization of the continuum being set to zero.

Schwarz & Clarke (1984) have computed the expected polarization of the continuum in the 400–700nm range due to hot spots. It appears that, whatever the temperature and extension of hot spots, polarization decreases with wavelength. We can then conclude that, in the case of 89 Her, the observed polarization across metal lines is not due to hot spots, as was theorized for Betelgeuse. We have found a polarization degree that is independent of wavelength; see Fig. 2.

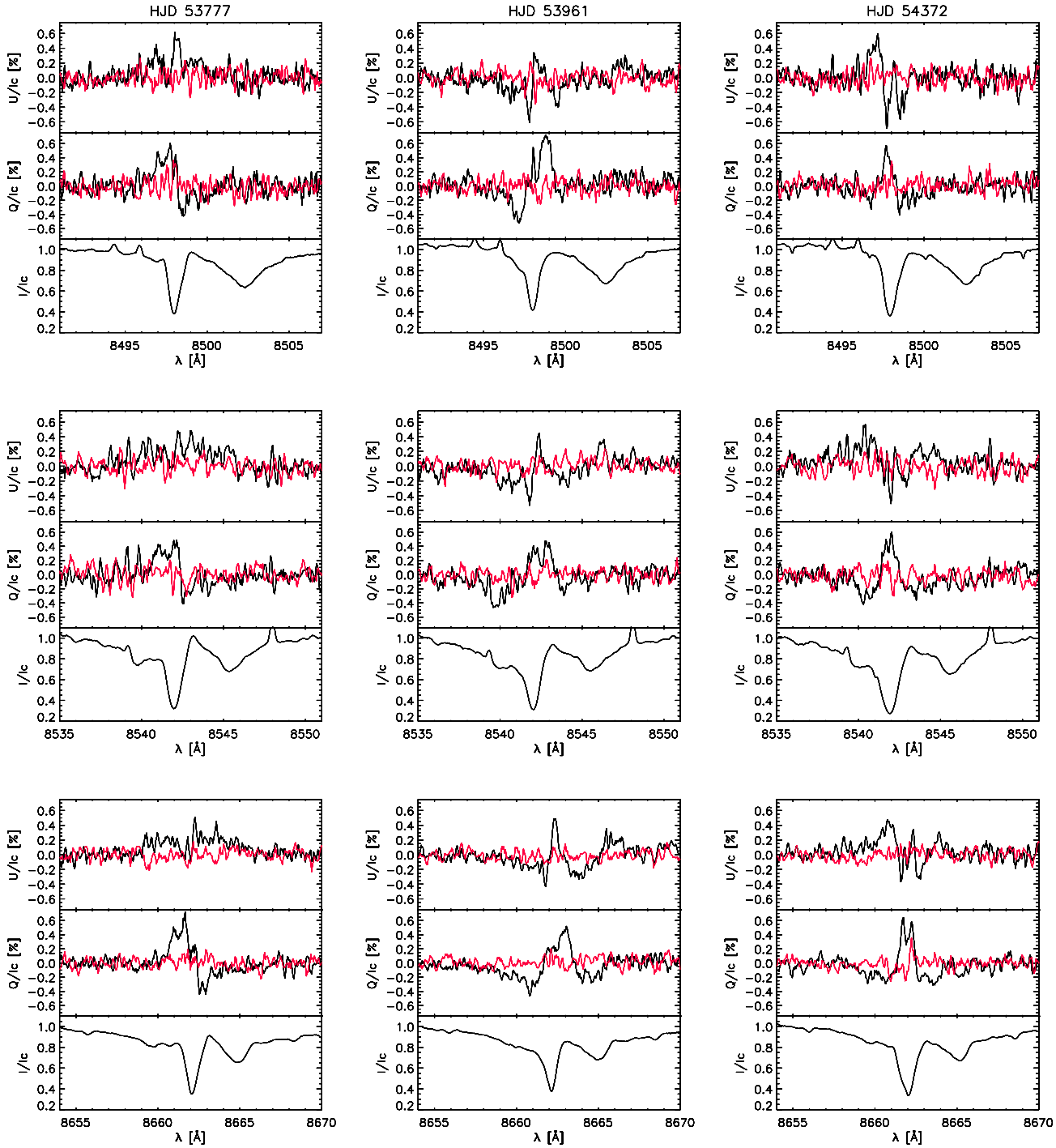


**Figure 8.** In black, the Stokes profiles of the IR calcium triplet as observed, from the left, on HJD 53777, 53961 and 54372. According to Kuhn et al. (2011), the very existence of polarization in the Ca II 8662-Å line, appearing equal to the other two lines, rules out scattering polarization from free electrons. It is compatible with optical pumping instead. In red are null profiles.

### *4.2.3 Scattering polarization from a bipolar outflow*

In Section 3.2, we explained the polarization of metal lines in emission by the presence of a circumbinary disc. Despite the detection of a 35–40per cent optical circumstellar flux contribution to the 89 Her luminosity by Hillen et al. (2013), polarization from free electrons of the circumbinary envelope is certainly not the origin of the polarization of metal lines in absorption. We have always detected linear polarization clearly across the Ca II 8662-Å line profile (Fig. 8), which, as pointed out by Kuhn, Geiss & Harrington (2011), cannot be due to scattering (Manso Sainz & Trujillo Bueno 2003).

Nevertheless, we have carried out numerical tests with the STOKES code to understand the role of scattering polarization from free electrons in the circumstellar environment. The variability of the polarization with orbital period rules out a scattering region much larger than the system orbit and we considered only a bipolar outflow. Indeed, polarized line profiles at the observed 1 per cent level

are predicted if the Hillen et al. (2013) bipolar outflow with an appropriate ($n_e \sim 10^{10}$–$10^{11}$ cm$^{-3}$) electron density is assumed. However, the ensuing 6 per cent polarized continuum is not compatible with the finding of Akras et al. (2017) of no polarization. In addition, we were not able to adapt the outflow properties in order to justify the polarization variability across spectral lines with the orbital period.

### 4.2.4 *Anisotropic radiation pumping*

Kuhn et al. (2007) suggested that the linearly polarized continuum of Herbig Ae/Be stars is due to *anisotropic radiation pumping*. To our knowledge, this mechanism has not yet been suggested as an origin of polarization in the metal spectral lines of stars other than the Sun. As to 89 Her, the presence of a very close (0.31 au, Bujarrabal et al. 2007) companion justifies, at least in principle, the assumption of a non-isotropic radiation field responsible for the observed polarized metal lines, which are seen to vary with the orbital period. A quantitative evaluation based on the anisotropy factor $w$ (Landi Degl'Innocenti & Landolfi 2004), which is zero for an isotropic radiation field and 1 for an unidirectional radiation beam, confirms the presence of a non-isotropic field between the two components of 89 Her. We obtain $w_{550nm} \sim 0.8$ if (1) we use the stellar parameters of Waters et al. (1993), who found that the primary component presents $T_{eff}$=6500 K, log $g$ = 1.0 and $R$=41 R$_\odot$, while the secondary is a 0.6-M$_\odot$ main-sequence star, i.e. an M0 V star with $T_{eff}$=4045 K, log $g$ = 4.6 and $R$=0.6 R$_\odot$ (Gray 2008), and (2) the surface fluxes of Kurucz (2005) and limb-darkening of Diaz-Cordoves, Claret & Gimenez (1995) are adopted.

As stated in the previous section, the polarization observed across the CaII 8662-Å line is evidence of optical pumping (Kuhn et al. 2011). Further direct proof of optical pumping would be the analysis of single line profiles. However, for single lines, the achived S/N ($\leq$400) was not enough to highlight the polarization and it was necessary to adopt the LSD method to produce a very high S/N ($10^3$–$10^4$, Table 1) *average line profile*. Unfortunately, with this method any information on the behaviour of single lines is lost. Despite this, we looked for spectral lines due to transition between levels with $J_{low} = 0$ and $J_{up} = 0$, which are expected to be unpolarized, or only slightly polarized if hyperfine structure is not neglected. Unfortunately, in the visible spectrum of 89 Her, the only one (namely YII 4422.258 Å) of these lines seen is not conclusive, since it is blended with the FeI 4422.568-Å line of comparable intensity.

To explore numerically the possibility that we are really in the presence of spectral line polarization induced by a periodically variable anisotropic radiation field due to the orbiting secondary, we compare synthetic Fe II 4508.288-Å Stokes profiles computed with the HAZEL code (Asensio Ramos, Trujillo Bueno & Landi Degl'Innocenti 2008) with the observed LSD profiles. For calculations, observed profiles have been corrected for Doppler shift due to the orbital motion of the primary component. Magnetic fields, which are not necessary to induce a population imbalance (Trujillo Bueno & Landi Degl'Innocenti 1997), have been neglected to minimize the free parameters to the following: (1) slab velocity $v_{sl}$, (2) thermal velocity $v_{th}$, (3) strength of the Stokes $I$ line $\eta_0$, (4) angle $\theta$ between the LoS and the normal $\boldsymbol{n}$ to the slab and (5) polarization angle $\gamma$, representing the azimuth of the polarization vector with respect to the north–south direction. Fig. 9 shows how the anisotropy factor $w$ and the angle $\theta$ contribute to the polarization level, again with the aim of minimizing the number of free parameters; the anisotropy

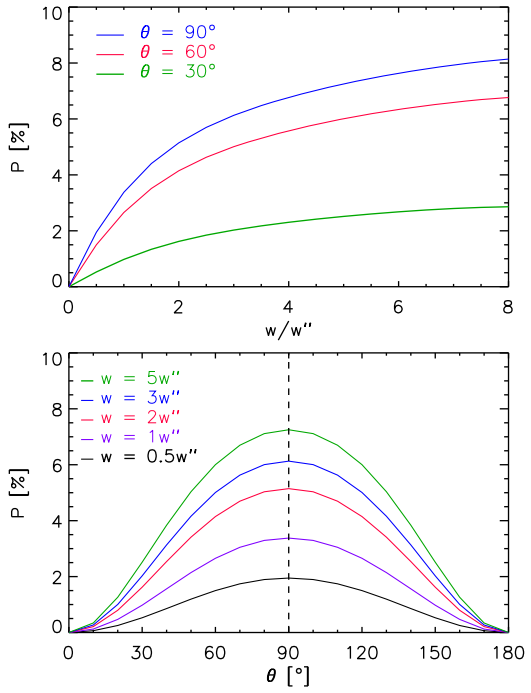


**Figure 9.** Spectral line polarization as a function of angle $\theta$ (bottom panel) and anisotropy factor $w$ (Landi Degl'Innocenti & Landolfi 2004), normalized to the Sun's value ($w'' = 0.37$) at 2 arcsec (top panel).

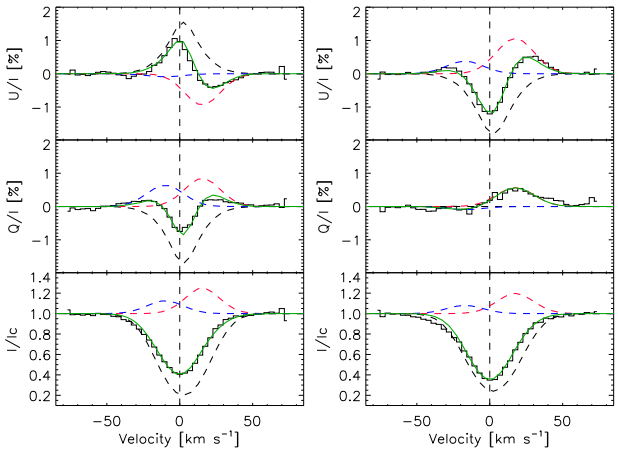


**Figure 10.** Example of CAOS-LSD profiles (black) fitted with three components (dashed lines). The solid (green) continuum is the sum of the three components. From the left, spectra were acquired on HJD 56816.515 and 56876.340 respectively.

factor has been arbitrarily fixed equal to the solar value ($w'' = 0.37$) at 2 arcsec.

Three slabs are required to fit the variable Stokes $Q/I$ and $U/I$ LSD profiles of 89 Her with HAZEL: a stationary feature in absorption (hereafter LINE 2 and due to SLAB 2) and two oppositely Doppler-shifted features, the blueshifted LINE 1 of SLAB 1 and the redshifted LINE 3 of SLAB 3. Fig. 10 shows an example of the fit for two CAOS-LSD profiles. With the exception of the thermal velocity $v_{th}$, which is constant in time, all fit parameters present a well-defined variability with the orbital period (Fig. 11).

According to the adopted ephemeris (equation 1), the radial velocity of the primary component of the 89 Her binary system

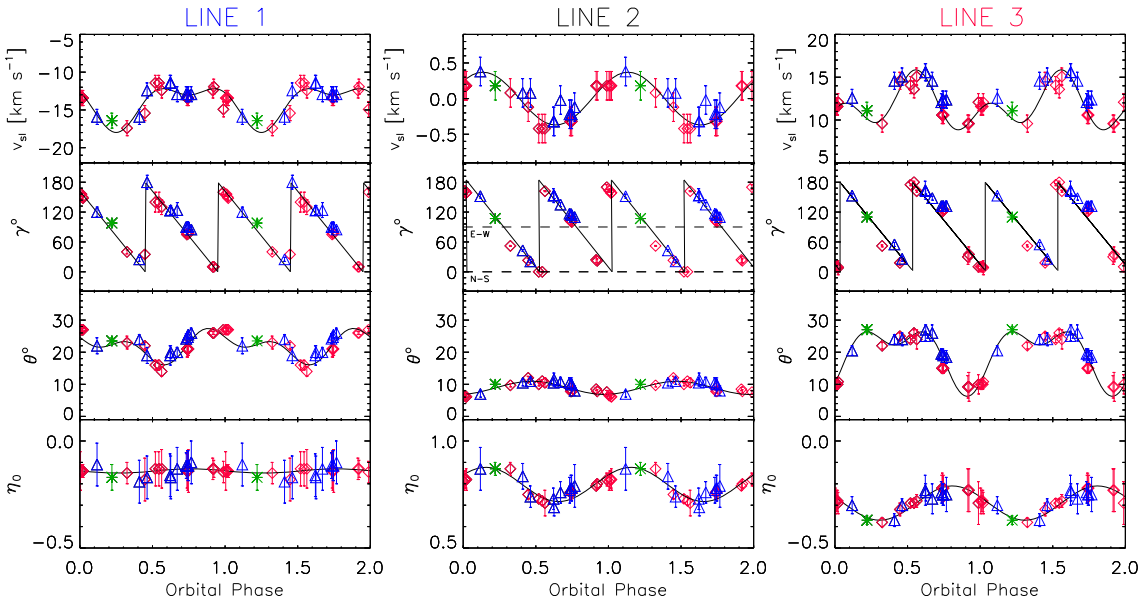


**Figure 11.** HAZEL parameters best matching the Stokes LSD profiles are folded with the orbital ephemeris given in equation (1). Symbols are as in Fig. 5. The sawtooth variation of the $\gamma$ angle, due to its definition in a 0–180° range, is indicative of a closed loop of the polarization vector along the orbital motion of the secondary star. The longitude of periastron $\omega = 359.3°$ (Waters et al. 1993) implies that the polarization vector is north–south oriented ($\gamma = 0°$) in conjunctions and east–west oriented ($\gamma = 90°$) in quadrature. Single and double wave variations have been assumed to match the parameter changes, except for the $\gamma$ one, which has been assumed linear in time.

presents its maximum at an orbital phase of zero when it moves away from us and the system is in quadrature. Thus the less massive secondary is before the primary (inferior conjunction) at phase 0.25, while the superior conjunction is at phase 0.75. Waters et al. (1993) measured a longitude of periastron $\omega = 359.3°$, orienting the main axis of the elliptical ($e = 0.189$) orbit in the east–west direction. Moreover, 89 Her is characterized by an hourglass structure that is orthogonal to the orbital plane, elongated in a direction that forms an angle of 15° with respect to the LoS and with a position angle of 45° (Bujarrabal et al. 2007). Fig. 12 shows a sketch of 89 Her.

We find that the overall behaviour of the fit parameters of the three slabs (Fig. 11) can be understood within the present picture of 89 Her: if the stationary SLAB 2 presents the *average* optical and physical properties of the primary component in reflecting and reprocessing radiation from the orbiting secondary, correspondingly the blueshifted SLAB 1 represents the jet pointing towards us and the redshifted SLAB 3 represents the receding jet. In such a hypothesis, it is straightforward to explain the following:

(i) the always negative SLAB 1 velocity and the always positive SLAB 3 velocity, both of the order of the hourglass expansion velocity, equal to ∼6–7 km s$^{-1}$ (Bujarrabal et al. 2007);

(ii) the constant thermal broadening, as expected for a phenomenon not due to a change of physical properties of the source, for example because of pulsations or spots;

(iii) the synchronous sawtooth variation of $\gamma$ angles for the three slabs with the orbital period. The continuous variation of $\gamma$, defined in the 0–180° range, shows that the polarization vector describes a closed loop in the sky, i.e. the scattering plane rotates around the LoS with the secondary star. The orientation of the polarization vector, aligned with the east–west direction in conjuctions and the north–

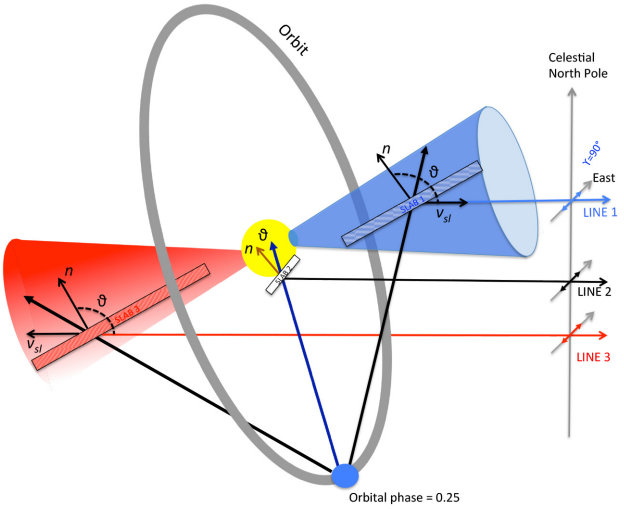


**Figure 12.** A (not to scale) sketch of 89 Her. The binary system presents a major axis aligned with the east–west direction (Waters et al. 1993). An hourglass structure is centred on the primary component and normal to the orbital plane (Bujarrabal et al. 2007). In the framework of anisotropic radiation pumping, the variable Stokes LSD profiles (Fig. 11) can be synthesized with the HAZEL (Asensio Ramos et al. 2008) code assuming three slabs: the stationary SLAB 2 presents the *average* optical and physical properties of the primary component in reflecting and reprocessing radiation from the orbiting secondary, correspondingly the blueshifted SLAB 1 represents the jet pointing towards us and the redshifted SLAB 3 represents the receding jet. $\theta$ is the angle between the normal $\boldsymbol{n}$ to the slab and the LoS, $v_{sl}$ the velocity of the slab towards the LoS. A complete description and definition of fit parameters are found in Section 4.2.4.

south direction in quadrature, is due to the east–west orientation of the major axis of the elliptical orbit (Figs 11 and 12).

A quantitative evaluation of the fit parameters and a description of their variability would require a 3-D version of HAZEL, which is not yet available, and a detailed knowledge of the 89 Her environment. Qualitatively, the variability of fit parameters is due to the imperfect symmetry with respect to the LoS, the non-null eccentricity of the orbit and absorption and occultation phenomena. For example, the weak modulation of SLAB 2 in $v_{\rm sl}$ and $\theta$ could be due to orbit eccentricity, or the large modulation of the SLAB 3 $\theta$ angle with respect to SLAB 1 could be a consequence of partial occultation of the receding jet by the primary star (Fig. 12).

## 5 CONCLUSIONS

On the basis of high-resolution spectropolarimetry, we have found that the metal lines of the binary system 89 Her are polarized as in the Second Solar Spectrum. These absorption metal lines with low excitation potentials present linear polarization, varying in time with the orbital period.

Because of the variability with orbital period, we rule out pulsations as the origin of the variability. Moreover, we can also rule out hot spots as the possible origin of continuum depolarization, because of the lack of dependence of polarization on wavelength.

According to Kuhn et al. (2011), the linear polarization we detected in the CaII 8662-Å line rules out scattering polarization from free electrons of the circumbinary environment and suggests that the origin of the Second Solar Spectrum we observed in 89 Her is the anisotropic radiation field due to the secondary star. In this framework, the periodic variability of polarized profiles, particularly the closed loop described by the polarization angle, can be ascribed to the jets at the basis of the hourglass structure being differently illuminated by the secondary orbiting around the primary.

A further unexpected property of 89 Her is the polarization across the emission metal lines. Numerical simulations show that polarized profiles are consistent with electron scattering in an undisrupted rotating disc. Such a disc appears to be rotated by 45° (clockwise) from the north–south direction, as observed by interferometric observations.

If it is possible to generalize the result of our observational campaign of 89 Her, we conclude that the inner regions of stellar enevlopes can be probed via high-resolution spectropolarimetry and that this appears to be the only diagnostic for stars still too far away for interferometric studies.

## ACKNOWLEDGEMENTS

This research used the facilities of the Canadian Astronomy Data Centre operated by the National Research Council of Canada with the support of the Canadian Space Agency. Based on observations made with the Italian Telescopio Nazionale Galileo (TNG) operated on the island of La Palma by the Fundación Galileo Galilei of the Istituto Nazionale di Astrofisica (INAF) at the Spanish Observatorio del Roque de los Muchachos of the Instituto de Astrofisica de Canarias.

## REFERENCES

Akras S., Ramírez Vélez J. C., Nanouris N., Ramos-Larios G., López J. M., Hiriart D., Panoglou D., 2017, MNRAS, 466, 2948
Arellano Ferro A., 1984, PASP, 96, 641
Asensio Ramos A., Trujillo Bueno J., Landi Degl'Innocenti E., 2008, ApJ, 683, 542
Asensio Ramos A., Martínez González M. J., Manso Sainz R., Corradi R. L. M., Leone F., 2014, ApJ, 787, 111
Aurière M. et al., 2016, A&A, 591, A119
Babcock H. W., 1947, ApJ, 105, 105
Bagnulo S., Wade G. A., Donati J.-F., Landstreet J. D., Leone F., Monin D. N., Stift M. J., 2001, A&A, 369, 889
Balick B., Frank A., 2002, ARA&A, 40, 439
Bujarrabal V., van Winckel H., Neri R., Alcolea J., Castro-Carrizo A., Deroo P., 2007, A&A, 468, L45
Clarke D., Schwarz H. E., 1984, A&A, 132, 375
Diaz-Cordoves J., Claret A., Gimenez A., 1995, A&AS, 110, 329
Donati J.-F., Semel M., Carter B. D., Rees D. E., Collier Cameron A., 1997, MNRAS, 291, 658
Donati J.-F., Catala C., Landstreet J. D., Petit P., 2006, in Casini R., Lites B. W., eds, Astronomical Society of the Pacific Conference Series Vol. 358, Solar Polarization 4. Astron. Soc. Pac., San Francisco, p. 362
Fabas N., Lèbre A., Gillet D., 2011, A&A, 535, A12
Gray D. F., 2008, The Observation and Analysis of Stellar Photospheres, Cambridge University Press, Cambridge
Gray R. O., Garrison R. F., 1989, ApJS, 69, 301
Harrington D. M., Kuhn J. R., 2009a, ApJS, 180, 138
Harrington D. M., Kuhn J. R., 2009b, ApJ, 695, 238
Hillen M. et al., 2013, A&A, 559, A111
Jordan S., Bagnulo S., Werner K., O'Toole S. J., 2012, A&A, 542, A64
Kipper T., 2011, Baltic Astronomy, 20, 65
Kruszewski A., Gehrels T., Serkowski K., 1968, AJ, 73, 677
Kuhn J. R., Berdyugina S. V., Fluri D. M., Harrington D. M., Stenflo J. O., 2007, ApJ, 668, L63
Kuhn J. R., Geiss B., Harrington D. M., 2011, in Kuhn J. R., Harrington D. M., Lin H., Berdyugina S. V., Trujillo-Bueno J., Keil S. L., Rimmele T., eds, Astronomical Society of the Pacific Conference Series Vol. 437, Solar Polarization 6. Astron. Soc. Pac., San Francisco, p. 245
Kurucz R. L., 2005, Mem. Soc. Astron. Ital. Suppl., 8, 14
Landi Degl'Innocenti E., Landolfi M. , 2004, Polarization in Spectral Lines, Astrophysics and Space Science Library Vol. 307, Kluwer Academic, Dordrecht
Lèbre A., Fabas N., Gillet D., 2011, in Johns-Krull C., Browning M. K., West A. A., eds, Astronomical Society of the Pacific Conference Series Vol. 448, 16th Cambridge Workshop on Cool Stars, Stellar Systems, and the Sun. Astron. Soc. Pac., San Francisco, p. 999
Lèbre A., Aurière M., Fabas N., Gillet D., Herpin F., Petit P., Konstantinova-Antova R., 2014, in Petit P., Jardine M., Spruit H. C., eds, IAU Symposium Vol. 302, Magnetic Fields throughout Stellar Evolution. Cambridge Univ. Press, Cambridge, p. 385–388
Leone F. et al., 2016a, AJ, 151, 116
Leone F., et al., 2016b, in Evans C. J., Simard L., Takami H., eds, Ground-based and Airborne Instrumentation for Astronomy VI, Vol. 9908, SPIE Proceedings, p. 99087K
Leone F., Catanzaro G., 2004, A&A, 425, 271
Leone F., Martínez González M. J., Corradi R. L. M., Privitera G., Manso Sainz R., 2011, ApJ, 731, L33
Leone F., Corradi R. L. M., Martínez González M. J., Asensio Ramos A., Manso Sainz R., 2014, A&A, 563, A43
Manso Sainz R., Trujillo Bueno J., 2003, Phys. Rev. Lett., 91, 111102
Martínez González M. J., Asensio Ramos A., Manso Sainz R., Corradi R. L. M., Leone F., 2015, A&A, 574, A16
McLean I. S., Coyne G. V., 1978, ApJ, 226, L145
Odell A. P., 1979, PASP, 91, 326
Odell A. P., 1981, ApJ, 246, L77
Osmer P., 1968, PASP, 80, 563
Roberts D. H., Lehar J., Dreher J. W., 1987, AJ, 93, 968
Sabin L., Wade G. A., Lèbre A., 2015, MNRAS, 446, 1988
Scargle J. D., 1982, ApJ, 263, 835
Schwarz H. E., Clarke D., 1984, A&A, 132, 370
Stenflo J. O., 1982, Sol. Phys., 80, 209

Tessore B., Lèbre A. Morin J., 2015, in Martins F., Boissier S., Buat V., Cambrésy L., Petit P., eds, SF2A-2015: Proceedings of the Annual meeting of the French Society of Astronomy and Astrophysics, Cambridge University Press, Cambridge, p. 429
Trujillo Bueno J., 2005, in Danesy D., ed., The Dynamic Sun: Challenges for Theory and Observations. Kluwer, Dordrecht, p. 7
Trujillo Bueno J., Landi Degl'Innocenti E., 1997, ApJ, 482, L183
Vink J. S., Harries T. J., Drew J. E., 2005, A&A, 430, 213
Wade G. A., Donati J.-F., Landstreet J. D., Shorlin S. L. S., 2000, MNRAS, 313, 823
Waters L. B. F. M., Waelkens C., Mayor M., Trams N. R., 1993, A&A, 269, 242
Wolff S. C., 1983, The A-type Stars: Problems and Perspectives, NASA, Washington, D.C.
Yan H., Lazarian A., 2008, ApJ, 677, 1401

This paper has been typeset from a TEX/LATEX file prepared by the author.